JETIR.ORG ISSN: 2349-5162 | ESTD Year : 2014 | Monthly Issue
JOURNAL OF EMERGING TECHNOLOGIES AND INNOVATIVE RESEARCH (JETIR)
An International Scholarly Open Access, Peer-reviewed, Refereed Journal

Ultra-Wide Band Slotted Tapered Vivaldi Antenna for RF Applications

Abhishek Choudhary, Deepak Sood
Department of Electronics and Communication Engineering,
University Institute of Engineering and Technology,
Kurukshetra University, Kurukshetra-136119, Haryana, India

Abstract: A novel configuration of Slotted Tapered Vivaldi Antenna over 0.8mm FR-4 substrate (61 mm × 48.4 mm) is designed. The antenna is simulated for 2-12 GHz for following configurations: conventional design, etching uniform constant length corrugations, etching double-sided exponentially decaying corrugations in spacing between uniform constant length corrugations, and, employing gratings in bore-sight direction. The measured -10dB bandwidth of antenna is 9.05 GHz that is from 2.95 to12 GHz. The final configuration of antenna provide a unidirectional pattern in the entire band with a maximum realized gain of 10.05 dBi at 8.5 GHz and maximum Front to Back Ratio of 24.67 dB at 4.5 GHz. The fabricated antenna shows flat Group Delay (ns) v/s Frequency (GHz) characteristics with an average value of 2.23 ns. The proposed design is useful for RF applications such as: RFID, radar systems, wideband transmission and reception from 2 to 12 GHz.

Keywords: UWD, Slotted Tapered Vivaldi Antenna , Conventional Slotted Tapered Vivaldi Antenna(CTSVA), Uniform Constant Length Corrugations (UCLCs), Double-Sided Exponential Corrugations (DSECs), Exponential Metallic Gratings (EMGs).

1.0 Introduction

The Ultra-Wide Band (UWB) antennas have versatile applications. Even a single UWB antenna can replace many narrow-band antennas combined together as it provide the required radiation pattern in the wide frequency band without losing its electrical characteristics and thereby leading to an overall inexpensive system with less weight and bulkiness, which may be employed in the smart airbags, automotive sensors, security sensors, Global Positioning systems, short-pulse generations etc. [1,2]. High data transmission rates with hundreds of Mega-bytes per second (Mbps) or several Giga-bytes per second (Gbps) may be achieved by designing the UWB antennas for the wireless applications [3-8]. The bandwidth of 3.1 - 10.6 GHz has been allocated by FCC for the UWB applications [9]. In contrast to other Ultra-Wide Band (UWB) antennas, Tapered Slot antennas exhibit narrow

beam-width, better gain characteristics, good time domain performance etc. [10]. The most commonly used class of Tapered Slot Antennas, i.e., the Slotted Tapered Vivaldi Antenna is basically a travelling wave end fire antenna which was proposed by Peter Gibson in 1979 [11] and has ease of impedance matching and highly directional characteristics over wide frequency band, low-cost in fabrication, which make it a prominent candidate for various applications such as microwave imaging [12], radar applications [13], civil engineering applications [14], breast cancer detection [15] etc. These applications may be covered by optimizing the Vivaldi Antenna so as to work in the desired frequency range. For the overall performance enhancement of the Vivaldi Antennas, many techniques have been reported in the literature [12-21], as listed in Table 1. It has been observed in some of the designs [14,17] that an enhancement in bandwidth is done at an expense of significant increase in size. Thus, the antenna must be modified in a way that overall compactness is not affected. In [12], non-uniformly decreasing corrugations are employed whereas in [19], an antenna design having the corrugations which are decreasing at a constant rate along with the metallic grating elements in slot area, acting as the directive elements for improving the gain in the bore-sight direction is employed. The corrugations, as well as the grating elements are reported to have enhanced the antenna performance.

In this proposed work, the design of a novel configuration of Tapered Slot Vivaldi Antenna, consisting of DSECs and EMGs is proposed. The simulation, along with rigorous optimization of parameters is done in four steps, where the comparison for simulation results of Return Loss (S_{11}) (dB) v/s Frequency (GHz) and Peak Realized Gain (dBi) v/s Frequency (GHz) of antennae is done using CST Microwave Studio. The S_{11} of final structure, for the same frequency range, is also verified by carrying out simulation using Ansys High Frequency Structure Simulator (HFSS), after which antenna is fabricated through chemical etching process. For the proposed antenna, the simulation of Radiation Efficiency as well as Front-to-back-Ratio is carried out. Also, for the fabricated antenna, the Forward Transmission Coefficient (S_{21}) (dB) v/s Frequency (GHz) and Group Delay (ns) v/s Frequency (GHz) are simulated, by keeping two identical antennae at a spacing of at-least Far-Field distance between them. The measurement of S_{11} v/s Frequency, S_{21} v/s Frequency and Group Delay v/s Frequency are done for proposed antenna using Agilent (now Keysight) PNA Network Analyzer N5222A. Finally, in a way similar to [14], the void detection in the concrete beam (by the means of observation in thhange Return Loss and Electric Field Distribution) is done by carrying out the numerical simulations in CST Microwave Studio for the proposed antenna.

Table 1 : Comparison with existing designs.

Reference	Antenna Size [L × W × h] (mm^3)	Substrate Material	Bandwidth (GHz)	Performance enhancement technique
[12]	62 × 50 × 1.52	Taconic RF-35 (ε_r = 3.5, tan δ = 0.0018)	1.96 - 8.61	Non - uniformly decreasing corrugation in a Tapered Slot Vivaldi Antenna
[13]	95 × 90 × 1.6	FR-4 (ε_r = 4.7, tan δ = 0.02)	0.069-0.25	Periodic dumbbell slots on both the edges

[14]	202 × 120 × 0.508	Rogers RO4003C (ε_r = 3.38, tan δ = 0.0027)	1.65 - 18	Antipodal Vivaldi Antenna with bends in inner edges and comb-shaped slits
[15]	62.6 × 32.5 × 1.6	FR-4 (ε_r = 4.4, tan δ = 0.025)	2.5 - 7.5	Radial Stub configuration for feeding purpose
[16]	46 × 40 × 0.8	Rogers RO4003 (ε_r = 3.55, tan δ = 0.0027)	3 - 11	Broadband gradient refractive index (GRIN) metamaterial as a lens for a Tapered Slot Vivaldi Antenna
[17]	258 × 210 × 1.5	FR4 (ε_r = 4.4, tan δ = 0.025)	0.22 - 6	Double Exponentially Tapered Slot Antenna (DETSA)
[18]	59.81×36.3× 0.64	Rogers RO3206 (ε_r = 6.15, tan δ = 0.0027)	4.73 -11	Palm-tree like Antipodal Vivaldi Antenna
[19]	45 × 40 × 0.8	FR4 (ε_r = 4.4, tan δ = 0.018)	2.9 - 12	Corrugations in slot area decreasing at constant rate along with grating elements in a Tapered Slot Vivaldi Antenna
[20]	36 × 36 × 0.8	FR4 (ε_r = 4.4, tan δ = 0.02)	3 - 12.8	Two - Pair Eye Shaped Slots in a Tapered Slot Vivaldi Antenna
[21]	120 × 80 × 0.75	F4B (ε_r = 2.65, tan δ = 0.001)	2.5 - 15	Double Slot Tapered Structure
Proposed Antenna :	61×48.4×0.8	*FR-4* (ε_r = 4.3, tan δ = 0.025)	~2.95-12	Constant length corrugations, double-sided exponentially decaying corrugations in spacing between them, grating elements in bore-sight direction

2.0 Evolution of Vivaldi Antenna design in various configurations

The Slotted Tapered Vivaldi Antenna is designed using double-sided copper clad FR-4 substrate, having a thickness of 0.8mm, the relative permittivity (ε_r) = 4.3 and loss tangent (tan δ) = 0.025. The simulation of antenna is done for a frequency range of 2-12 GHz using CST Microwave Studio Suite in four steps in which CTSVA is modified in a way for obtaining the Vivaldi Antenna with enhanced performance as shown in Figure 1(a)-(d). Fig 1(e) shows the employed feeding mechanism and Figure1(f) gives the used colour code for the materials.

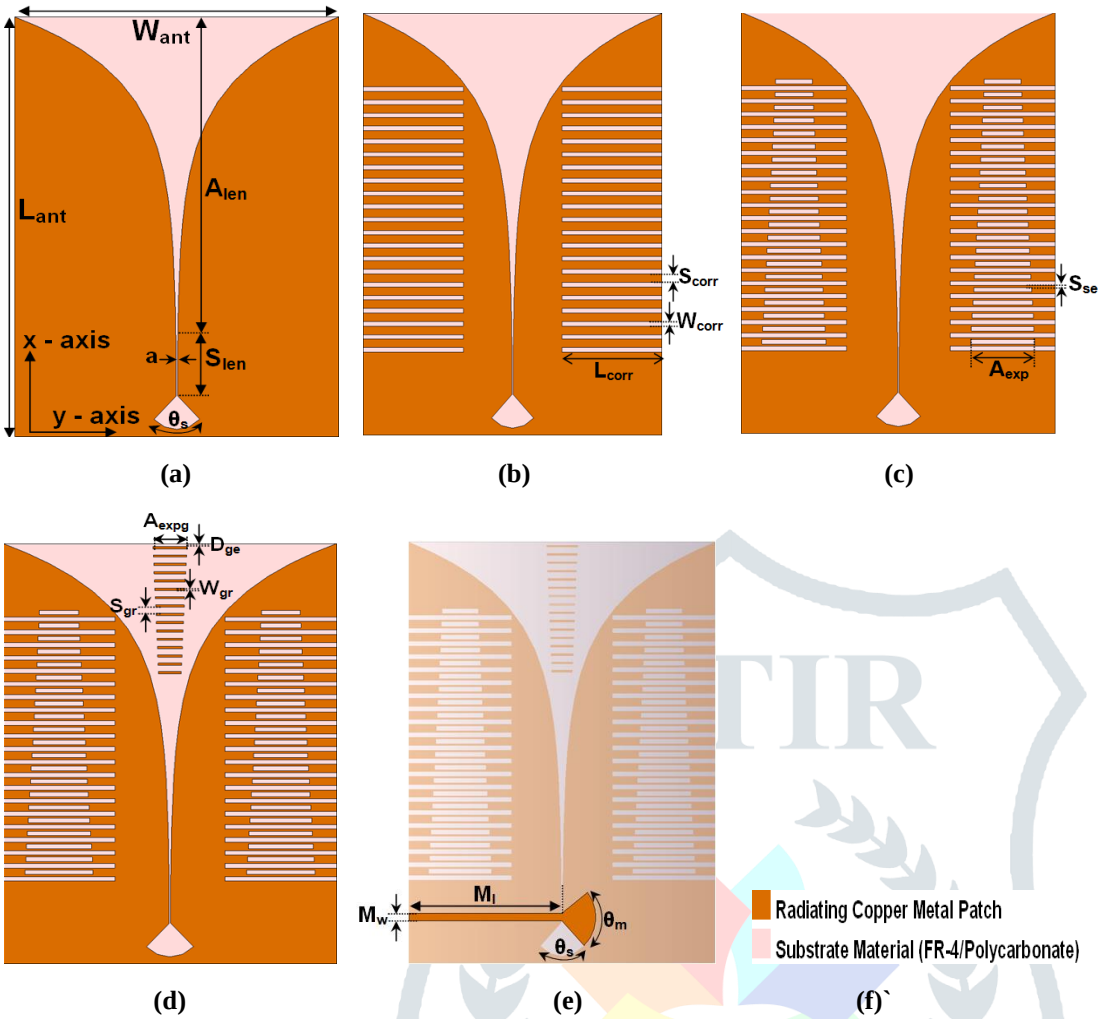

Figure 1 : Schematics of Vivaldi Antenna Design Evolution : (a) CTSVA, (b) CTSVA with UCLCs (c) CTSVA with DSECs in the spacing between UCLCs, (d) CTSVA with DSECs in spacing between UCLCs along-with EMGs in bore-sight direction , (e) Feeding Mechanism, (f) Colour Code for Metal Patch and Substrate Material

For the design of Vivaldi Antenna, the 35 µm copper based micro-strip to slot-line transition [24], opposite to the bore-sight direction is designed for feeding the antenna, which is designed in a way similar to [13] for a wide-band impedance matching as shown in Figure 1(e), where the optimization of arc angles , 'θ_s' for the slot-line and ' θ_m' for the micro-strip line is done along with the micro-strip length (M_l) and micro-strip width(M_w) for obtaining a perfect 50Ω impedance matching over a broad frequency range. The minimization of reflections from the micro-strip to slot-line transition is done through the open-circuited angular cavity. The evolutions in antenna design are as follows:

(i) Design (i): CTSVA: In this configuration, the radiating copper metal patch follows an exponentially tapered profile as shown in Figure 1(a). The length of slot-line is taken as 'S_{len}', after which tapering, i.e., exponential flaring starts and goes on till antenna's extreme edge, i.e., towards the antenna's bore-sight direction. Taking the Equations 1-3 in a way similar to [19], if 'a' is the slot width of antenna and 'b' is a constant, as in Equation 3 and ' o_r' is the opening rate of tapered slot, calculated as per Equation 4, then the double-sided tapering profile for the antenna is given by $v(t)$:

$$v(t) = \pm\, be^{o_r t} \quad \text{(For t : 12.8 mm to 61 mm)} \qquad (1)$$

($v(t)$ is positive for the right side of radiating patch and negative for its left side)

where, $b = \frac{a}{2}$ (2)

and the opening rate ' o_r' is :

$$o_r = \frac{1}{A_l} ln\left(\frac{W_{ant}}{a}\right) \quad (3)$$

(ii) Design (ii) : CTSVA with UCLCs : The etching of uniform, constant length corrugations is done from the outer edges on left as well as right side of copper radiating patch area of the antenna as shown in Figure1(b). These corrugations have constant length (L_{corr}) and width (W_{corr}) values and a uniform spacing (S_{corr}) between them. A comb-like structure is represented by these corrugations, which is symmetric on both the sides of the antenna in a way similar to [14]. Acting as high impedance region, the corrugations concentrate the maximum surface current within the inner edges of the tapered, exponential portion of the patch. The etching of these corrugations over the patch is done in a way that these cover maximum area in the patch and overall antenna is also compact. The etching of total 21 such corrugations is done.

(iii) Design (iii) : CTSVA with DSECs in the spacing between UCLCs : In the spacing between the corrugations of the previous design, exponentially decaying corrugations, from the top as well as bottom sides, are etched as shown in Figure1(c). These have a maximum amplitude as (A_{exp}) and width is same as that of the corrugations in previous design, i.e., W_{corr} and are spaced of S_{se} between alternate corrugations of previous design. These newly employed corrugations are exponentially decaying, from the top as well as bottom sides on the right as well as the left of the radiating metallic patch. The exponential profile of these newly designed corrugations is given by Equation 4. If we consider 'r' as the exponentially decaying rate of the newly designed corrugations where 'i' varies from 0 to 21, we have:-

$$f(i) = \pm A_{\exp}\, e^{-ri} \quad (4)$$

($f(i)$ is positive for the right side of radiating patch and negative for its left side)

A similar design approach was employed in [19], where the uniformly decreasing corrugations (decreasing from one top as well as bottom sides) are etched so as to improve the antenna performance by surface current concentration towards the inner edge of the antenna, thereby reducing side-lobes level. In this design, the effect of uniform and constant length corrugations is combined with the exponentially decaying corrugations (top and bottom exponential decay) on the right as well as left sides of radiating metal patch. The combined effect of constant as well as the exponentially decaying corrugations leads to a better surface current concentration. An added advantage of double sided exponential corrugations is that now the surface current's direction is changed

from both the sides, and it is concentrated towards the inner edge of tapered slot in much better way, thereby reducing the side lobes and back lobe radiations.

(iv) Design (iv) : CTSVA with DSECs in spacing between UCLCs along-with EMGs in bore-sight direction : Along with the side lobes reduction, an overall improved response in the higher frequency region is obtained by placing copper grating elements over the substrate in the bore-sight direction, which are exponential in nature on top as well as bottom sides and thus have different dimensions for each grating shown in Figure1(d). The peak amplitude of these metallic gratings is 'A_{expg}' and width is 'W_{gr}'. A total of 16 such grating is employed where the last grating is at a distance, D_{ge} from the bottom portion of antenna and the spacing between two consecutive gratings is given as S_{gr}. A relation between the peak amplitudes and width of the metallic gratings with the parameters of exponentially decaying corrugations is there so as to maintain a symmetry in the design which is given by Equations 5-6 :

$$A_{expg} = \frac{A_{exp}}{2} \quad (5)$$

$$W_{gr} = \frac{W_{corr}}{2} \quad (6)$$

Taking i : 0 to 16, the exponential profile for the gratings is given by Equation 7 :

$$g(i) = A_{\text{expg}}\, e^{-ri} \quad (7)$$

These gratings act in a way similar to directive elements in Yagi- Uda Antenna for improving the overall radiation in the bore-sight direction and thus reducing side lobes level and thereby enhancing the unidirectional nature of Vivaldi Antenna. The optimized dimensions are as shown in Table 2:

Table 2 : Optimized simulated parameter values of different configurations of Vivaldi Antenna

Parameter	Value	Parameter	Value
L_{ant}	61 mm	A_{exp}	9.97 mm
W_{ant}	48.4 mm	r	0.012
a	0.25 mm	D_{ge}	0.52 mm
o_r	0.0944	A_{expg}	4.985 mm
A_{len}	48.2 mm	θ_s	90^0
S_l	6.47 mm	θ_m	90^0
L_{exts}	6.33 mm	M_l	24.2 mm
L_{corr}	16 mm	M_w	1.47 mm
W_{corr}	0.64 mm	W_{gr}	0.32 mm
S_{corr}	1.2 mm	S_{gr}	1.04 mm
S_{se}	0.28 mm	----------	----------

3.0 Simulation Results (for comparison of antenna configurations)

The simulation is done in CST Microwave Studio for the frequency range of 2-12 GHz, covering S- , C- and X-Band radar frequencies. The comparison of simulation results, after optimization, for Return Loss (S_{11}) and Peak Realized Gain (dBi) v/s Frequency (GHz) is done for all the four antennae configurations as follows:

3.1 Return Loss (dB) v/s Frequency (GHz) plot

The simulated Return Loss (S_{11}) (dB) v/s Frequency (GHz) for the antenna configurations is shown in Figure 2. As observed from the simulated Return Loss (dB) v/s Frequency (GHz) plot, -3 dB bandwidth for all four antenna evolutions is almost 2-12 GHz. While analyzing for -10 dB bandwidth, for Design (i), multiple bands are observed, whereas, Antenna No. (ii), (iii) and (iv) show nearly same -10 dB bandwidth. The observed bandwidths through the plot for antenna designs, Design (i)-(iv) are given in Table 3 :

Table 3 : Bandwidth comparison of antenna evolutions

Antenna Design	-10 dB bandwidth	-3 dB bandwidth
Antenna No. (i)	2 GHz - 2.06 GHz, 3.11 GHz - 4.16 GHz, 4.86 GHz - 9.63 GHz	2 GHz - 12 GHz
Antenna No. (ii)	2.62 GHz - 9.76 GHz	2.08 GHz - 12 GHz
Antenna No. (iii)	2.6 GHz - 9.83 GHz	2.08 GHz - 12 GHz
Antenna No. (iv)	2.61 GHz - 9.55 GHz	2.09 GHz - 12 GHz

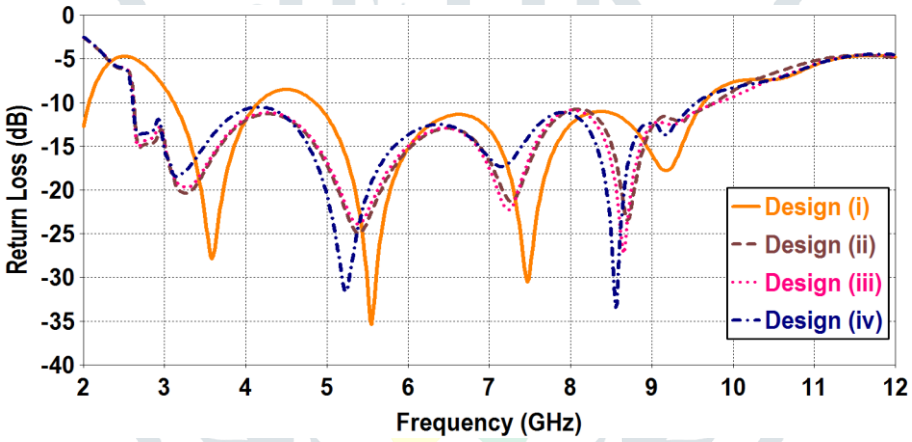

Figure 2 : Simulated Return Loss v/s Frequency plot

3.2 Peak Realized Gain v/s Frequency plot

The simulated Return Loss (S_{11}) (dB) v/s Frequency (GHz) for the antenna configurations is shown in Figure 3. As it is observed from the plot, for over 55% of the optimized frequency range, the value of Peak Realized Gain is maximum for Design (iv). The maximum values for the covered radar frequency bands are :-

- S-Band : 6.52 dBi at 3.5 GHz;
- C-Band : 9.84 dBi at 7.5 GHz;
- X-Band : 10.05 dBi at 8.5 GHz.

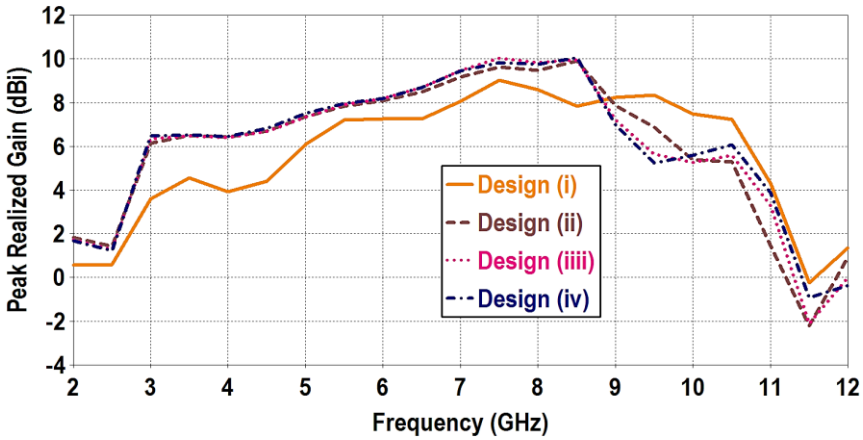

Figure 3 : Simulated Peak Realized Gain v/s Frequency plot

3.3 Surface Current Density distribution

The simulated Surface Current Density distribution (A/m) is given in Figure 4. The logarithmic colour scale is taken so as to display the distribution more clearly. Also, the patch and substrate colours are taken as black and white respectively so as to avoid the inter-mixing with the colours scale of surface current distribution. It is observed that the maximum surface current is found in the portion of exponential taper and the area of radial stubs. It is desirable to concentrate the maximum surface current from the outer edges of the exponential tapered slot to the inner edges, thereby reducing the level of side lobes, which is achieved by modifying the antenna configuration. The etching of corrugations lead to a better confinement the Surface Current Density within the inner edges of the radiating metal patch. Due to new type of corrugations in Figure 4(c), the Surface Current Density direction changes from the top as well as bottom sides, thereby helping in the concentration of surface current. In the final design as shown in Figure 4(d), the grating elements are employed, acting as directive elements in Yagi-Uda antenna, so as to give the overall enhanced radiation characteristics in the bore-sight direction. It is clearly observed that there is a concentration of the Surface Current Density, due to which the speed of the electrons carrying current is reduced and thereby reducing the overall magnitude of Surface Current Density as we modify the design of antenna.

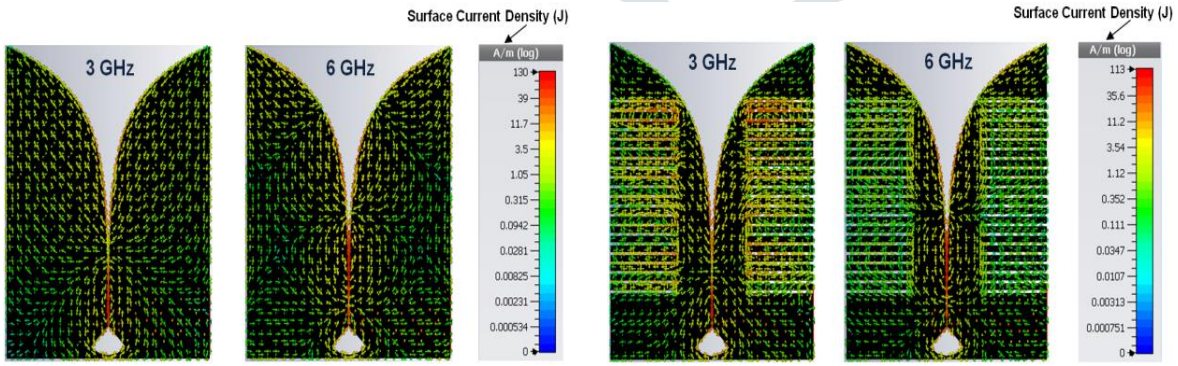

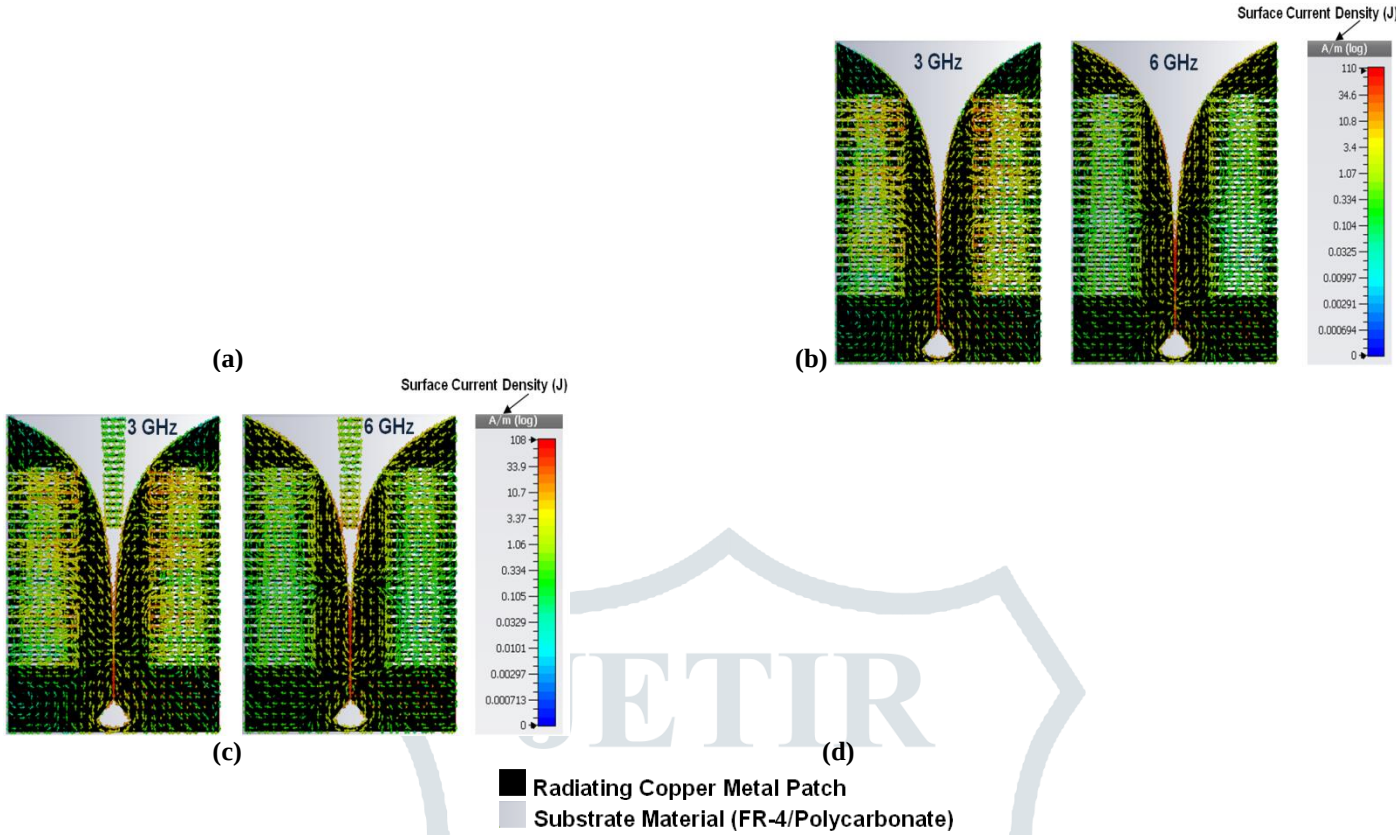

Figure 4 : Simulated Surface Current Density Distribution : (a) For Design (i), (b) For Design (ii), (c) For Design (iii), (d) For Design (iv), (e) Colour Code for antenna

3.4 2D Radiation Plots

The simulated 2D Far-Field Radiation Plots for antennae configuration evolutions at different frequencies are shown in Figure 5. For the analysis of plots, the antenna's bore-sight direction is pointing towards the vertical position and the co-ordinates in CST Microwave Studio are taken as $z' \leftrightarrow x$, $x' \leftrightarrow y$, $y' \leftrightarrow x$ (x -, y-, z-representing the co-ordinates in global co-ordinate system of CST Microwave Studio and x' -, y'-, z'- are taken are local coordinates for analysis). Here, theta(θ) varies from 0^0 to 360^0 for fixed value of Phi(ϕ). The cases of Co-Polarization ($\phi = 0^0$) and Cross-Polarization ($\phi = 90^0$) are taken. As it is clearly observed from the plots, the design modification leads to a better unidirectionality of antenna and also the level of side-lobes is reduced.

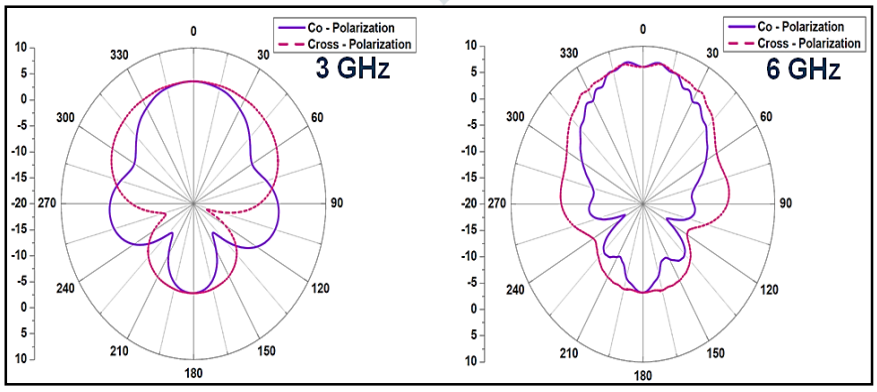

(a)

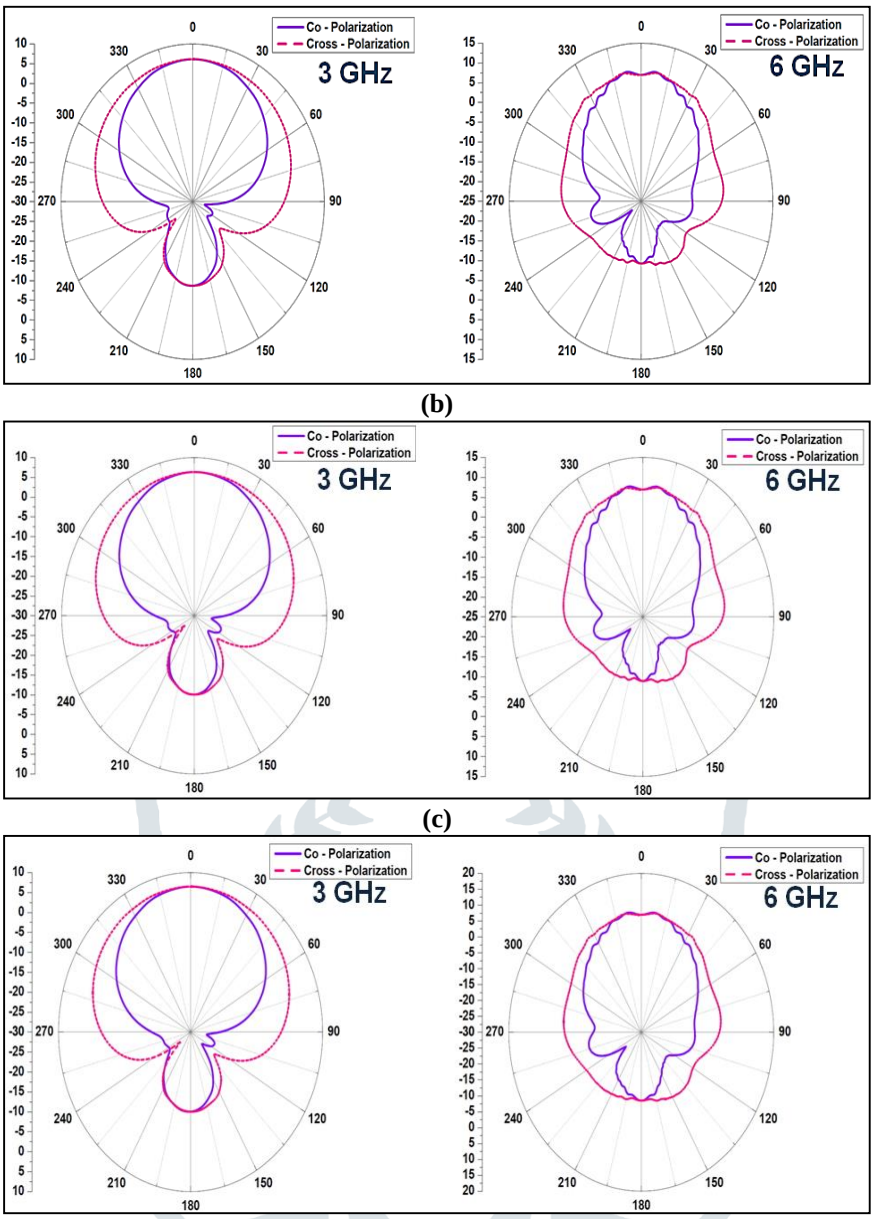

Figure 5 : Simulated 2D Radiation Plots (in terms of Peak Realized Gain) : (a) For Design (i), (b) For Design (ii), (c) For Design (iii), (d) For Design (iv)

3.5 Simulated Radiation Efficiency and Front to Back Ratio v/s Frequency (GHz) plot (for proposed antenna)

The simulated Radiation Efficiency (%) and Front to Back Ratio(dB) v/s Frequency (GHz) plot is shown in Figure 6. Moderate values of Front to Back Ratio and Radiation Efficiency are observed. The maximum value of Radiation Efficiency and Front to Back Ratio for different radar frequency bands within the optimized frequency range of 2-12 GHz are given in Table 4.

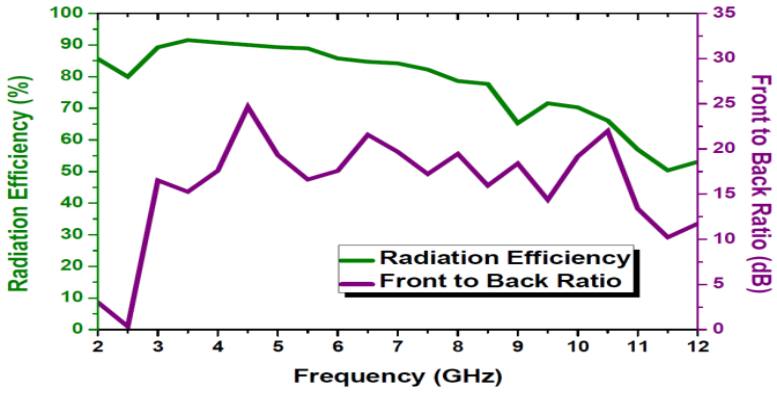

Figure 6 : Simulated Radiation Efficiency and Front to Back Ratio v/s Frequency plot

Table 4 : Maximum Simulated Percentage Radiation Efficiency and Front to Back Ratio for the Radar Bands within optimized frequency range for FR-4 based antenna

Radar Frequency Band	Maximum Radiation Efficiency(%)	Frequency (GHz)	Maximum Front to Back Ratio (dB)	Frequency (GHz)
S - Band	91.57 %	3.5	17.57	4
C - Band	90.77 %	4	24.67	4.5
X- Band	78.63 %	8	21.98	10.5

4.0 Fabrication and Measurements (and some other simulated results of proposed antenna)

The prototype of antenna as shown in Figure 7 is fabricated by chemical etching process on a double-sided copper clad FR-4 substrate, having a thickness of 0.8mm, the relative permittivity (ε_r) = 4.3 and loss tangent (tan δ) = 0.025.

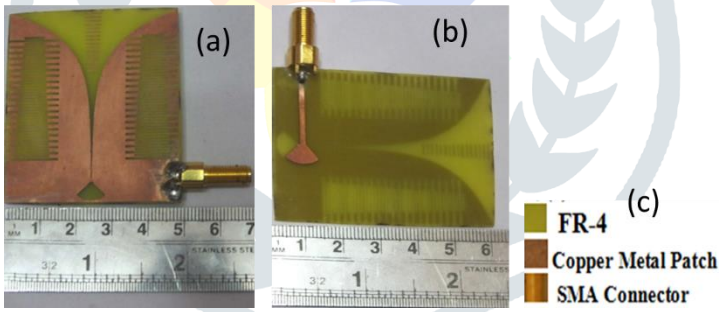

Figure 7 : Fabricated antenna configuration : (a) Top View, (b) Bottom View, (c) Colour Code

4.1 Measurement Setup

The measurements for the Return Loss (S_{11}) (dB), insertion loss (S_{21}) (dB) and Group Delay (ns) v/s Frequency (GHz) for both the antenna configurations are carried out using Agilent (now Keysight) Performance Network Analyzer N5222A. The measurement setup is shown in Figure 8 :

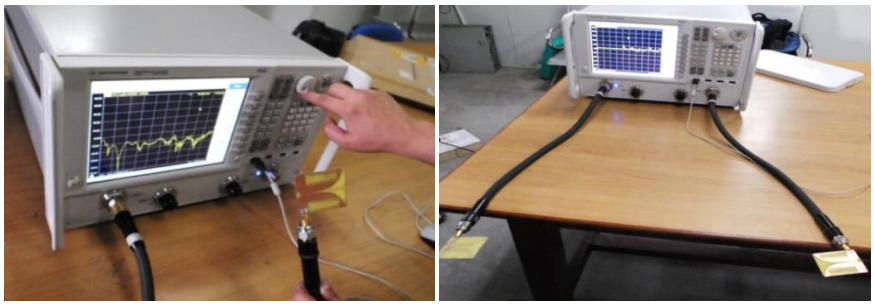

(a) **(b)**

Figure 8: Measurement Setup : (a) For Return Loss v/s Frequency, (b) For Forward Transmission Coefficient and Group Delay v/s Frequency

4.2 Measured Return Loss (S_{11}) v/s Frequency plot (with comparison to simulated results)

The measured Return Loss (S_{11}) (dB) v/s Frequency (GHz) plot for the FR-4 based antenna is shown in Figure 9. The simulated results of return losses are also verified by simulating same structure in Ansys HFSS. The bandwidths found after the measurements are given in Table 5.

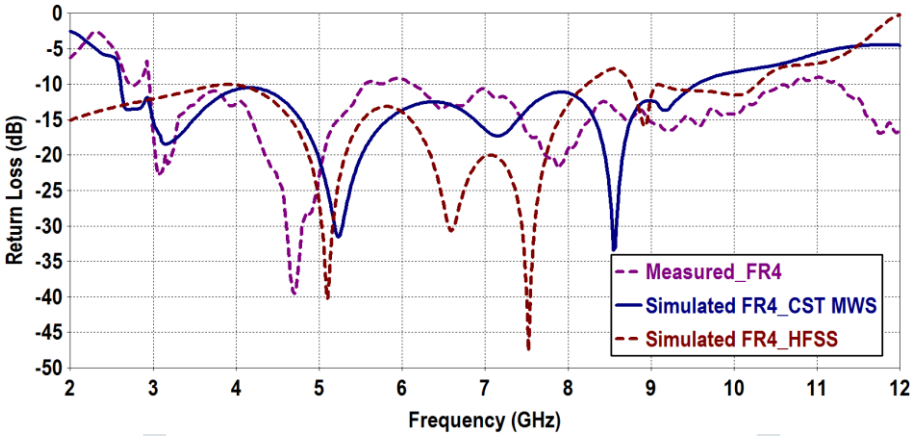

Figure 9 : Comparison of Simulated and Measured Return Loss v/s Frequency plot

Table 5 : Simulated and measured bandwidths for proposed antenna

Type of Result	-10 dB bandwidth	-3 dB bandwidth
Simulation (CST MWS)	2.61 GHz - 9.55 GHz	2.09 GHz - 12 GHz
Simulation (HFSS)	2 GHz - 8.22 GHz and 8.75 GHz - 10.28 GHz	2 GHz - 11.66 GHz
Fabrication	≈ 2.95 GHz -12 GHz	≈ 2GHz - 12 GHz

4.3 Measured insertion losses (S_{21}) (dB) v/s Frequency plot and Measured Group Delay v/s Frequency plot (and their comparison with simulated results) :

The **insertion losses (S_{21})** quantifies the amount of power transferred from 1 to 2 port, i.e., port of Antenna 1 to port of Antenna 2. The measurement for the **insertion losses (S_{21})** (dB) v/s Frequency (GHz) was done by keeping the antennas in the face-to-face orientations (i.e., the bore-sight directions of both antennas pointing each other). The antennas are kept at a distance which is more than the Far-Field distance of antenna, i.e., at 34 cm from each other.

Also, considering for a UWB Antenna like Vivaldi Antenna, which could be employed in the pulse-band communications, microwave imaging and radar applications, in addition to frequency domain performance a good time domain performance is desired. The distortion in time is measure through Group Delay (ns) v/s Frequency (GHz) plot. For these measurements, two identical antennas are kept facing each other. Since the Network Analyzer doesn't directly give the output file for the group delay plot in nanoseconds(ns), the calculations are carried out using the Phase angle of the Forward Transmission Coefficient (S_{21}) v/s Frequency (GHz) plot. As per the results shown in Figure 10, nearly flat group delay is observed while comparing simulation and fabrication results. The average measured group delay is 2.23 ns. The comparison plot for simulated and measured S_{21} v/s Frequency is given in Figure 10 and that for Group Delay v/s Frequency in Figure 11.

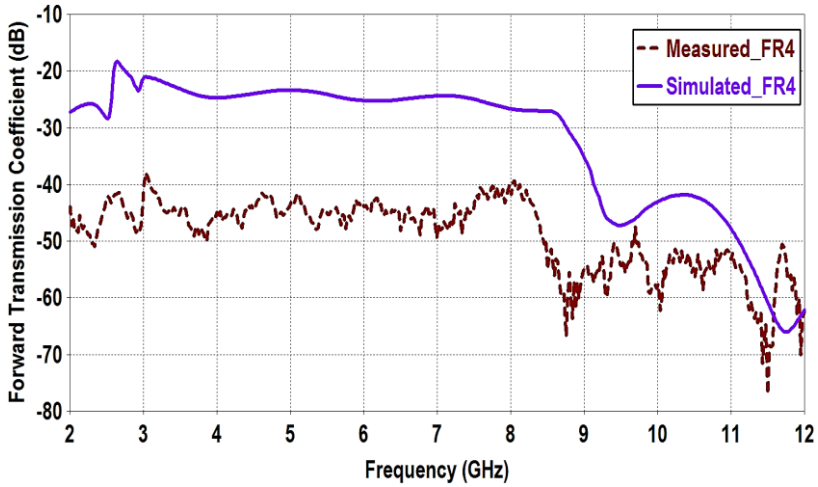

Figure 10 : Comparison of Simulated and Measured Forward Transmission Coefficient v/s Frequency plot

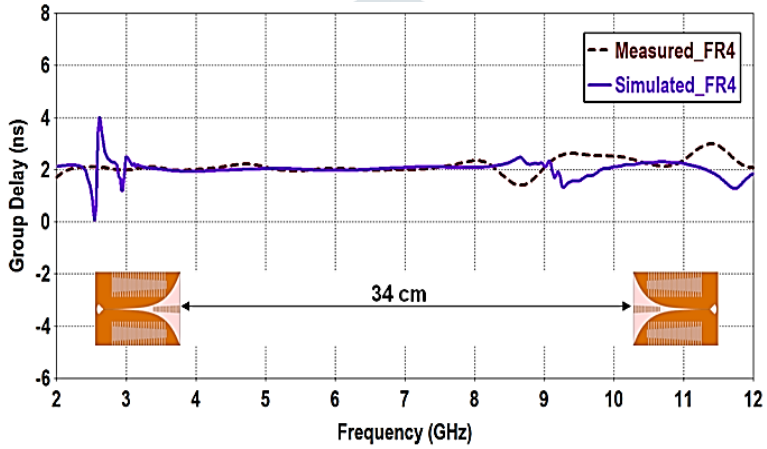

Figure 11 : Comparison of Simulated and Measured Group Delay (ns) v/s Frequency (GHz) plot

7.0 Conclusion

The design of a compact novel configuration of UWB Vivaldi Antenna is done over 0.8 mm FR-4 substrate with outer dimensions as 61 mm × 48 mm. In the modified configuration, i.e., the proposed antenna, the constant length as well as exponential corrugations act as resistive loads which help in the concentration of the surface current. Also there are directive elements, i.e., the gratings, which help in directing the radiation in the boresight direction, with the reduction in the level of side lobes. The measured S_{11} for the proposed antenna show that the -10 dB bandwidth is 2.95-12 GHz. The maximum simulated Peak Realized Gain of 10.05 dBi is observed at 8.5 GHz. The proposed antenna has moderate valued simulated Radiation Efficiency, ranging 50.36 % - 91.57 % over the entire frequency band The Front to Back Ratio of proposed antenna is positive over the optimized frequency range with a maximum of 24.67 dB at 4.5 GHz, which further signifies the maximum radiation in the forward direction. Also, the group delay, which is an essential parameter in characterizing the UWB antennas is nearly flat over the entire frequency band for FR-4 (averaged at 2.23 ns). The measured Forward insertion loss is good over the entire optimized frequency range. Thus, the proposed antenna, working in 2-12 GHz band may potentially be employed

for use in the S-, C- and X-Band Radar applications and also cover UWB frequency range of 3.1-10.6 GHz which make it useful for RFID applications.

8.0 References

[1] Siwiak, K., Mc. Keown, D., (2004). Ultra-Wideband Radio Technology, John Wiley & Sons, Ltd, Chapter 2, 30-31.

[2] Rahayu, Y., Rahman, T. A., Ngah, R., Hall, P. S., (2008). Ultra wideband technology and its applications. 5th IFIP International Conference on Wireless and Optical Communications Networks (WOCN '08), Surabaya, 1-5.

[3] Oppermann, I., Hamalainen, M., Iinatti, (2004). UWB Theory and Applications. John Wiley & Sons, Ltd.

[4] Bala, R., Marwaha, A., (2016). Development of computational model for tunable characteristics of graphene based triangular patch antenna in THz regime. Journal of Computational Electronics. 15(1), 222–227.

[5] Bala, R., Marwaha, A., Marwaha, S., (2016). Performance enhancement of patch antenna in terahertz region using graphene. Current Nanoscience. 12(2), 237-243.

[6] Bala, R., Marwaha, A., Marwaha, S., (2016). Comparative analysis of zigzag and armchair structures for graphene patch antenna in THz band. Journal of Materials Science: Materials in Electronics. 27(5), 5064-5069.

[7] Bansal, G., Marwaha, A., Singh, A., Bala, R., Marwaha, S., (2018) Graphene based Wideband Arc Truncated Terahertz Antenna for Wireless Communication. Current Nanoscience, Bentham Science, 14, 1-8.

[8] Bala, R., Marwaha, A., (2016). Characterization of graphene for performance enhancement of patch antenna in THz region. Optik-International Journal for Light and Electron Optics. 127(4), 2089-2093.

[9] Federal Communication Commission, First order and report: Revision of part 15 of the Commission's rules regarding UWB transmission systems (2002).

[10] Yngvesson, K.S., Korzeniowski, T. L.,. Kim, Y. S, Kollberg, E. L., and Johansson, J. F. (1989) The tapered slot antenna-a new integrated element for millimeter-wave applications. IEEE Transactions on Microwave Theory and Techniques.37(2), 365-374

[11] Gibson P.J., (1979) The Vivaldi Aerial. 9th European Microwave Conference, Brighton, UK, 101-105.

[12] Abbak, M., Akıncı, M. N., Çayören, M., Akduman, I. (2017) Experimental Microwave Imaging With a Novel Corrugated Vivaldi Antenna. IEEE Transactions on Antennas and Propagation. 65(6), 3302-3307.

[13] Elsheakh, D. M., Abdallah, E. A., (2014), Compact shape of vivaldi antenna for water detection using ground pentrating radar. Microw. Opt. Technol. Lett., 56: 1801-1809.

[14] Mahdi M., Kharkovsky, Sergey, Case, Joseph, T., Samali , Bijan (2017) Antipodal Vivaldi antenna with improved radiation characteristics for civil engineering applications. IET Microwaves, Antennas & Propagation.11(6), 796-803.

[15] Lazaro, A. , Villarino, R., and Girbau, D., (2011), Design of Slotted Tapered Vivaldi Antennafor UWB breast cancer detection. Microw. Opt. Technol. Lett. . 53, 639-643.

[16] Singha R, Vakula D., (2018) Gain enhancement of the ultra-wideband tapered slot antenna using broadband gradient refractive index metamaterial. Int J RF Microw Comput Aided Eng. . 28(2), 1-10.

[17] Zhang, F., Fang, G. Y., Ji, Y. C., Ju, H. J., Shao, J. J., (2011). A Novel Compact Double Exponentially Tapered Slot Antenna (DETSA) for GPR Applications IEEE Antennas and Wireless Propagation Letters. 10,195-198.

[18] Oliveira, A. M. D., Perotoni, M. B., Kofuji S. T., Justo J. F. (2015). A palm tree antipodal Vivaldi antenna with exponential slot edge for improved radiation pattern. IEEE Antennas Wireless Propag. Lett., 14, 1334–1337.

[19] Kumar Pandey, G., and Kumar Meshram, M., (2015). A printed high gain UWB vivaldi antenna design using tapered corrugation and grating elements. Int J RF and Microwave Comp Aid Eng, 25, 610-618.

[20] Ma, K., Zhao, Z.Q., Wu, J.N., Ellis, M.S., Nie, Z.P. (2014) A printed vivaldi antenna with improved radiation patterns by using two pairs of eye-shaped slots for UWB applications, Prog Electromagn Res 148, 63–71.

[21] Wang, G.M., Wang, X.J., Gao, Zhou, C., (2013) Double-slot Vivaldi antenna with improved gain, Electron Lett 49 , 1119–1121.

[22] Shuppert, B., (1988) Microstrip/Slotline Transitions: Modeling and Experimental Investigation. IEEE Trans. on Microwave Theory and Techniques. 36(8), 1272-1282.

[23] Knott, E., F., (1993). Dielectric Constant of Plastic Foams. IEEE Transactions on Antennas and Propagation. 41(8), 1167-1171